II -4-5-2. Interpretation

Magnetic leneaments were extracted using the aboub mentioned figures and were illustrated in Fig. II -4-6. The aeromagnetic survey was revealed quite effective for extract structural elements over the survey area covered by thick calcrete. The survey area could be subdivided into three terrains based upon the magnetic characteristics as follows.

(1)Terrain exposed or underlain by the basement complex at a shallow depth

(2)Terrain occupied by thick Damara sediments

(3)Terrain underlain by Karoo basalt

A swarm of magnetic lineaments traverse the three terrains with varying length and width. Some of them are associated with faults. The southeast of the area is characterized by short-wave magnetic pattern indicating shallow emplacement of the basement complex. It seems that thin Damara sediment overlies the basement. The magnetic anomaly patterns suggests the basement stepping down towards northwest by east-north east trending faults as well as dome structure interpreted by long-wave pattern. Thick Damara sequence may overly the deep seated basement complex here.

Potential stratigraphic boundary could be traced because of faint contrast of magnetic susceptibility, in spite of totally low susceptibility of Damara sediments.

II-4-6. Measurement of Physical Property

II-4-6-1. Objective and Number of Samples

The physical properties of samples collected both from host lithologies and ore material were measured. The property measured included magnetic susceptibility, induced polarization and resistivity. Some seventy five samples were measurement for magnetic susceptibility and thirty four samples were examined for all of the properties. The time domain method was used to measure for induced polarization and resistivity.

The heterogeneity of the properties on a micro scale and the off situ measurement of samples may not necessarily reflect the true field values, however, the properties are important in indicating expected trends. This will guide the interpretation of the survey and hence the methods to be used in the geophysical exploration programme of Phase II.

II-4-6-2. Equipment and Sample preparation

(1)Magnetic susceptibility

The magnetic susceptibility meters used were the compact and light KAPAMETER and BISON magnetometer whose capabilitys are shown in Table II -4-1. The KAPAMETER is highly sensitive and is designed for both measurement in the field and in the laboratory. However, for laboratory measurements large samples are required and the Bison-type

PRODUCTION SUMMARY

Date	Day	Flt	Hrs	Lkms	Details
24 Sep	Sun			0	Lanseria - Windhoek Tsumeb
25 Sep	Mon			0	Set up, buy equip etc.
26 Sep	Tues	1,2,3	2.00	194	Comp performed in am. Flt 2 aborted due to constant system resets.
27 Sep	Wed	4,5,6	8.00	1328	No problems
28 Sep	Thu	7	5.20	1245	Late start due to extending of GPS antennna by 4 metres
29 Sep	Fri	8,9	7.10	1432	No problems
30 Sep	Sat	10	8.00	1428	No problems
01 Oct	Sun	11	8.00	1638	No problems
2 Oct	Mon	-	0.00	0	Pilots rest day
3 Oct	Tues	12	7.90	1623	No problems
4 Oct	Wed	13	8.00	1705	No problems
5 Oct	Thu	14	8.00	1705	Alternator blows on landing - return to Lanseria for MPI and repairs.
6 Oct	Fri		0.00	0	Lanseria
7 Oct	Sat		0.00	0	Lanseria
8 Oct	Sun		0.00	0	Lanseria
09 Oct	Mon	-	5.00	0	Lanseria - Grootfontein - Tsumeb
10 Oct	Tues		0.00	0	Starter u/s, engineer from Windhoek - fixed
11 Oct	Wed	15,16	9.10	1608	No problems
12 Oct	Thu	17,18	10.50	2235	No problems
13 Oct	Fri	19,20,21	8.10	1439	Check on heading, Compensation
14 Oct	Sat	-	0.00	0	Change fuel pump
15 Oct	Sun	22	5.70	1003	Hydraulic u/s
16 Oct	Mon	-		0	Unable to take off due to hyd.pipe
17 Oct	Tues	-		0	Tsumeb - Windhoek
23 Oct	Mon	23	2.9	553	Windhoek - Tsumeb
24 Oct	Tues	24, 25	10.21	2213	No problems
25 Oct	Wed	26,27	11.5	2435	Weather turbulent
26 Oct	Thur	28,29	11.45	2475	Weather turbulent
27 Oct	Fri	30	8.1	1203	End of survey

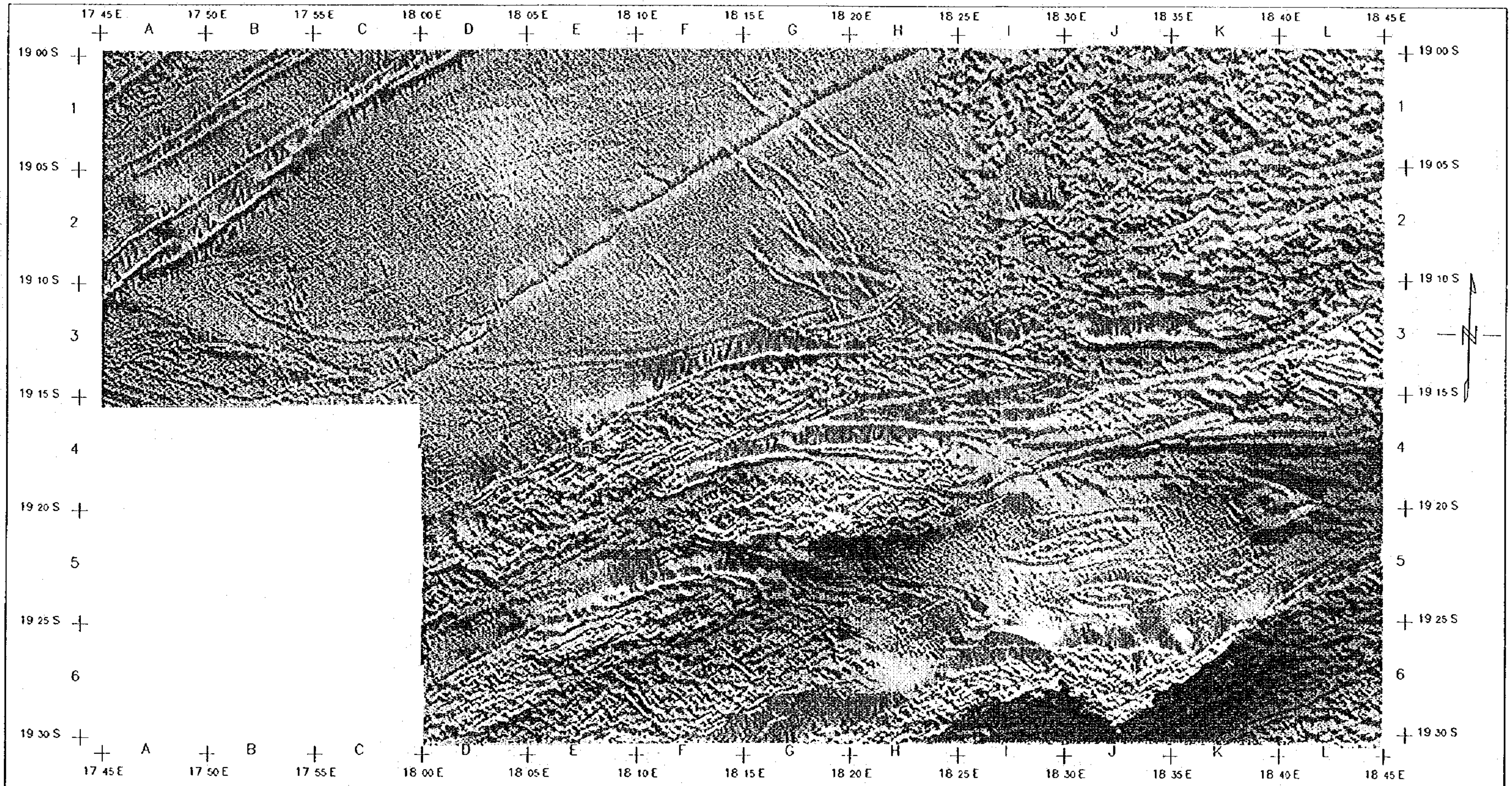

Scale 1:250000

5000 0 5000 10000 15000

(metres)

Fig. II - 4 - 5

MAGNETIC IMAGE PROCESSING PRODUCT

OTAVI MOUNTAINLAND PROJECT
(MARCH 1996)

M. M. A. J.

magnetometer was thus used for smaller samples. The measurements were then corrected for sample surface as well as shape and the susceptibility readings were then converted into SI unit. (1 SI=4 π cgs)

(2)IP Value(Chargeability) and Resistivity

The equipment used is shown in Table II −4−1. The samples measured for polarization and resistivity were trimmed into cubes of approximately five−centimetre and these were submerged into water for about one day prior to measurement. All samples except those from drill cores were measured in three dimensions. The sampling time and interval to mid point against channel number are shown below.

Channel No.	4	5	6	7	8	9	10	11	12	13	14
Width(msec)	20	40	40	80	80	140	140	230	230	360	360
Mid-Point(")	60	90	130	190	270	380	520	705	935	1230	1590

II−4−6−3. Results of Measurement

The results of magnetic susceptibility are presented in Table II −4−3. Each of IP and resistivity values are geometric means of the three dimensional values. The IP values recorded from channel M4 to M14. The three dimensional values of the anisotropic samples are also shown in the same table. Channel number 12, which is most commonly used as standard, was used for this data interpretation.

II−4−6−4. Interpretation of magnetic susceptibility data

The susceptibility distribution of the formations and lithological facies is shown in Fig. II −4−7. The mean value in the figure signifies the geometric mean. Based upon the results obtained from laboratory measurements and the aeromagnetic anomaly map the following conclusions can be drawn.

<1> The magnetic susceptibility of the rocks in the area in decreasing in the following order: Karoo dolerite, Grootfontein Metamorphic Complex, Mulden Group sediment, and finaly Otavi Group sediment.

<2> The susceptibility of calcrete is relatively low, indicating that the calcrete, regardless of

<3> A Karoo dolerite coincides with northeast trending linear structure in Fig II −4−5. A swarm of lineaments in the mid−central part of the area are also interpreted as dolerite dykes.

<4> The next ranked are the basement rocks which cause high magnetic anomalies in the south of the survey area.

<5> The Damara sequence is significantly lower compared to the first two and is magnetically transparent. However, the dolomites of Tsumeb Subgroup shows such a low magnetic susceptibility that it causes a vague contrast against the slightly higher susceptible shale and sandstone of Mulden Group. Nevertheless, the possible Paleokarst hosts for ore deposit may be identified by this method.

<6> Among the ore minerals, chalcocite and iron oxides show comparatively higher magnetic susceptibility compared to the Mulden sandstone. If an slightly massive ore deposit is hosted by a sediment with extremely low magnetic susceptibility, a weak and small but discernible magnetic anomaly can be formed.

II-4-6-5. Data analysis of Resistivity and Induced Polarization(Chargeability)

(1) Principle of IP method

When a current is introduced underground, a series of electrochemical phenomena would occur within the constituent particles. Two of these phenomena are detected by the IP method, and these are described below.

Over voltage effect : The current introduction gives rise to an electric double layer on the sulphide or metallic conductive substance and the current interruption causes a discharge in the opposite direction of introduction. This phenomenon is an effect of combination of ionic conduction with electronic conduction and this thus enables the IP method to be effective for minerals with electronic conductivity.

Normal effect or Background : The effect is the varying polarization occurring in rocks when a current is introduced. This is brought about mainly by membrane polarization of the small quantity of clay included in the pores of rocks. Amongst the clay minerals, montmorillonite shows the most intense effect whereas kaolinite shows the weakest. The membrane polarization reaches the maximum value when the volume ratio of clay to rock is as much as 5 percent, and it decreases as far from the value. The maximum value of close to 5 percent for montmorillonite is translated into approximately 2 percent in terms of FE value and is small enough if compared to Over Voltage effect.

The observed IP effect is termed polarization ratio or chargeability and is expressed as Vs(tn)/Vp(mV/V). The polarization ratios of the Frequency method and the Time Domain Method give experimental values of 1 percent and 5 mV/V respectively.

(2) Analysis of observed values

The correlation between resistivity and polarization(chargeability) is evident from the observed values(Fig. II -4-8). In this figure, the following thresholds were identified:

Table II－4－3 Geophysical Properties of Samples (1)

Sample No.	Rock,Mineral name	Form. code	Physical properties Mag.sus. *1E-3 SI	Resistivity Ω·m	IP(M12) mV/V
101	Calcrete	Tk	0.03		
102	Calcrete	Tk	0.09		
103	Calcrete	Tk	0.04	1,904	2.11
104	Calcrete	Tk	0.05	910	0.00
105	Dolerite	Jd	31.06		
106	Dolerite(core)	Jd	* 25.50	28,338	7.28
107	Sandstone(pseudo aplite)	Md	0.04	5,189	2.55
108	Fine sandstone	Md	* 0.37	22,149	12.66
109	Fine sandstone	Md	* 0.56	19,021	1.44
110	Medium sandstone (fine pyrite)	Md	* 0.27	13,621	3.00
111	Brn silt phyllite	Md	0.19		
112	Shale(fine pyrrhotite)	Md	* 1.29	20,249	11.04
113	Shale	Md	* 0.44	10,783	18.87
114	Sandy chert	Md	0.05		
115	Blk calc sandstone	Nt	0.01		
116	Phyllite	Nt	0.60		
117	Blk dolomitic shale	Nt	0.10		
118	Calc blk shale	Nt	0.03		
119	Black shale	Nt	0.01	1,868	0.56
120	Red to grey oolitic chert	Nt	0.03	13,295	6.49
121	Blk chert	Nt	0.03		
122	Dolomite	Nt	0.01		
123	Msv dolomite	Nt	0.01		
124	Dolomite	Nt	0.41		
125	Dolomite	Nt	0.04		
126	Dolomite chert alt gry brn dol	Nt	0.04		
127	Fractured dolomite	Nt	0.03		
128	Sericite dolomite	Nt	0.07		
129	Dolomite	Nt	0.08	14,048	0.93
130	Dolomite with calcite	Nt	0.02		
131	White dolomite	Nt	0.01	21,403	1.12
132	Dark dolomite	Nt	0.10	16,056	0.51
133	Dolomite(carbonaceous)	Nt	0.01	24,196	3.42
134	Calc sandstone	Na	0.05	9,640	9.38
135	Shale	Na	0.44	894	1.40
136	Black shale	Na	0.12		
137	Shale	Na	0.04	8,866	1.69
138	Calcitized dolomite or limestone	Na	0.29		
139	Limestone	Na	0.04	29,154	-0.37

* Bison magnetic susceptibility meter

Tk:Kalahari Formation Td:Karoo Dolerite Md:Mulden Group Nt:Tsumeb Subgroup Na:Abenab Subgroup

Table II－4－3 Geophysical Properties of Samples (2)

Sample No.	Rock,Mineral name	Form. code	Physical properties Mag.sus. *1E-3 SI	Resistivity Ω·m	IP(M12) mV/V
140	Calc silicate rock	Nc	0.01		
141	Dolomite limestone blk shale alt.	Nc	0.00		
142	Chlorite schist with Cu mineral	Nc	0.77		
143	Calc silicate chlorite schist	Nc	0.19		
144	Arkose sandstone	Nn	0.09		
145	Sandstone iron formation	Nn	2.10		
146	Arkose sandstone-conglomerate	Nn	0.08		
147	Arkose sandstone	Nn	0.06	14,322	4.51
148	Banded fragmental folded limestone	Nn	0.01	25,282	0.01
149	Mica schist	Mgr	21.32		
150	Psammitic schist	Mgr	0.20	3,218	4.32
151	Amphibolite schist	Mgr	1.80	2,239	1.37
152	Predamara basement granite	Mgr	1.12		
153	Drk red quartzite	Mgr	3.33		
154	Gneissose sandstone	Mgr	15.96		
155	Plagioclase porphyritic granite	Mgr	1.00	2,568	4.82
156	K-feldspar porphyritic gneiss	Mgr	26.00		
157	Aplitic facies	Mgr	1.74		
158	Basic intrusive?	Mgr	1.29		
159	Basic dyke rock (boulder)	Mgr	0.72		
160	Basic dyke rock	Mgr	5.29		
161	Green hornblende rock	Mgr	3.74		
162	Chalcocite ore	Ore	2.68	19.30	231.98
163	Chalcocite ore	Ore	0.36	9050.82	11.08
164	Chalcopyrite-bornite ore	Ore	0.39	40.56	508.59
165	Chalcopyrite in sandstone	Ore	0.12	174.00	249.92
166	Chalcopyrite-galena ore	Ore	0.05	93.30	315.11
167	Galena-sphalerite ore	Ore	0.09		
168	Galena in host rock	Ore	0.03	3,412	39.29
169	Galena ore	Ore	0.09	118.6	549.16
170	Galena ore	Ore	0.09	224	543.88
171	Pb-Zn type mineralisation MVT	Ore	0.03		
172	Vanadium mineral	Ore	0.04	10,203	1.31
173	Vanadium mineral in calcite	Ore	0.15		
174	Fe-Mn ore	Ore	2.51		
175	Malachite in quartz vein	Ore	0.26	104.2	240.47

Nc:Chuos Formation Nn:Nosib Group Mgr:Grootfontein Basement Complex

Table II − 4 − 4 Acquired Values of Resistivity and IP of Samples

Sample No.	Rock,Mineral name		Resistivity Ω·m	Electric property (Each value is 3D geometric mean except core sample data and negative value) IP property M=4	5	6	7	8	9	10	11	12	13	14
103	Calcrete		1903.73	10.82	8.83	7.27	6.11	5.11	4.18	3.37	3.03	2.11	1.69	1.39
104	Calcrete		910.43	2.26	1.67	1.31	1.09	0.78	0.53	0.34	0.13	0.00	-0.05	-0.12
106	Dolerite	core	28337.65	33.01	27.89	23.65	19.75	16.37	13.47	11.01	8.98	7.28	5.87	4.68
107	Sandstone(pseudo-aplite)	core	5189.46	13.41	11.17	9.38	7.73	6.31	5.12	4.11	3.25	2.55	1.98	1.51
108	Fine sandstone	core	22148.67	64.74	54.89	46.38	38.43	31.46	25.39	20.32	16.08	12.66	9.85	7.59
109	Siltstone-fine sandstone	core	19021.47	7.28	6.03	5.08	4.17	3.35	2.67	2.10	1.63	1.44	0.89	0.33
110	Medium sandstone (fine pyrite)	core	13621.29	12.56	10.59	9.04	7.61	6.38	5.32	4.42	3.65	3.00	2.47	2.02
112	Shale(fine pyrrhotite)	core	20249.29	37.65	33.31	29.43	25.59	22.03	18.74	15.84	13.26	11.04	9.13	7.53
113	Shale	core	10782.58	86.84	73.90	62.80	52.44	43.44	35.64	29.10	23.48	18.87	15.05	11.96
119	Black shale	1	746.51	7.67	6.57	5.63	4.71	3.89	3.11	2.49	2.14	1.71	1.33	0.96
		2	9056.89	4.31	3.38	2.71	2.14	1.65	1.25	0.93	0.69	0.48	0.35	0.23
		3	963.33	3.51	2.51	1.81	1.34	0.95	0.66	0.44	0.34	0.21	0.17	0.22
		avg	1867.51	4.88	3.82	3.03	2.38	1.83	1.36	1.01	0.80	0.56	0.43	0.36
120	Red to grey oolitic chert		13295.14	21.10	18.73	16.67	14.59	12.67	10.87	9.22	7.76	6.49	5.39	4.41
129	Dolomite		14047.84	6.81	5.44	4.43	3.54	2.78	2.15	1.65	1.25	0.93	0.68	0.48
131	White dolomite		21402.93	4.43	3.75	3.29	2.82	2.41	2.02	1.69	1.38	1.12	0.89	0.71
132	Dark dolomite		16056.16	4.55	3.53	2.82	2.20	1.69	1.27	0.94	0.70	0.51	0.36	0.24
133	Dolomite(carbonaceous)		24196.29	14.82	12.74	11.07	9.42	7.85	6.45	5.31	4.24	3.42	2.71	2.03
134	Calc sandstone		9640.32	53.53	44.46	36.92	30.07	24.27	19.37	15.36	12.05	9.38	7.24	5.54
135	Shale	1	494.12	13.53	10.84	8.84	7.11	5.57	4.11	3.02	2.02	1.32	1.04	0.59
		2	598.69	20.14	16.78	13.99	11.56	9.23	7.36	6.32	4.58	3.68	2.52	2.03
		3	2418.46	10.25	7.68	5.75	4.16	2.94	2.04	1.39	0.91	0.57	0.33	0.17
		avg	894.38	14.08	11.18	8.92	6.99	5.33	3.95	2.98	2.03	1.40	0.96	0.59
137	Black shale		8865.54	17.90	13.71	10.59	8.02	6.00	4.45	3.27	2.35	1.69	1.19	0.82
139	Limestone		29154.30	0.20	-0.12	-0.25	-0.36	-0.35	-0.38	-0.41	-0.42	-0.37	-0.33	-0.29
147	Arkose sandstone		14321.55	16.72	14.53	12.61	10.78	9.20	7.81	6.53	5.46	4.51	3.69	3.04
148	Banded fragmental folded limestone		25281.91	1.53	1.04	0.77	0.55	-0.37	0.24	0.13	0.06	0.01	-0.03	-0.06
150	Psammitic schist		3218.47	15.88	13.81	12.08	10.41	8.88	7.51	6.30	5.25	4.32	3.56	2.89
151	Amphibolite schist		2239.29	7.48	6.15	5.18	4.26	3.47	2.79	2.24	1.76	1.37	1.05	0.78
155	Plagioclase porphyritic granite		2568.26	19.87	17.08	14.76	12.51	10.54	8.75	7.21	5.86	4.82	3.89	3.12
162	Chalcocite ore		19.30	457.41	432.75	407.54	378.90	349.15	318.50	288.83	259.66	231.98	206.08	182.44
163	Chalcocite ore	1	14512.83	28.02	24.34	22.08	19.34	16.79	14.39	12.22	10.30	8.62	7.20	5.99
		2	8561.02	16.71	14.56	12.78	11.06	9.52	8.13	6.91	5.82	4.91	4.11	3.42
		3	5967.42	105.27	94.30	83.91	73.26	63.25	54.01	45.76	38.43	32.11	26.66	22.06
		avg	9050.82	36.66	32.43	28.72	25.02	21.63	18.49	15.69	13.21	11.08	9.24	7.67
164	Chalcopyrite-bornite ore		40.56	933.39	899.45	860.21	811.16	756.62	696.37	634.53	570.78	508.59	447.95	390.12
165	Chalcopyrite in sandstone	1	61.13	928.64	896.59	860.77	817.43	770.41	719.57	668.00	615.40	564.00	513.93	466.76
		2	58.73	968.60	937.50	902.46	859.59	812.49	760.78	707.52	652.14	597.39	543.09	491.35
		3	1467.13	139.87	124.90	111.26	97.71	85.23	73.76	63.55	54.36	46.33	39.27	33.19
		avg	174.00	501.07	471.75	442.13	409.47	376.46	343.07	310.84	279.42	249.92	222.13	196.72
166	Chalcopyrite-galena ore	1	62.09	845.34	808.44	766.45	714.85	658.57	597.98	537.55	477.55	421.31	369.04	322.49
		2	57.97	689.38	647.00	601.22	548.55	494.68	440.77	390.25	342.84	300.30	262.00	228.37
		3	225.63	660.12	617.50	570.79	515.88	458.55	400.04	344.64	292.95	247.32	207.63	174.27
		avg	93.30	727.29	686.11	640.72	587.03	530.60	472.43	416.59	363.33	315.11	271.79	234.13
168	Galena in host rock		3411.55	112.48	101.98	92.15	81.97	72.24	62.92	54.36	46.41	39.29	32.90	27.33
169	Galena ore		118.59	452.82	659.66	611.72	831.83	780.25	724.16	666.68	607.33	549.16	491.56	428.41
170	Galena ore		223.70	833.84	796.81	882.68	834.95	782.38	724.64	665.38	604.10	543.88	484.53	424.21
172	Vanadium mineral		10203.36	6.44	5.33	4.50	3.75	3.09	2.52	2.04	1.54	1.31	1.03	0.80
175	Malachite in quartz vein		104.19	506.97	475.19	443.30	408.32	373.11	337.64	303.66	270.87	240.47	212.24	186.76

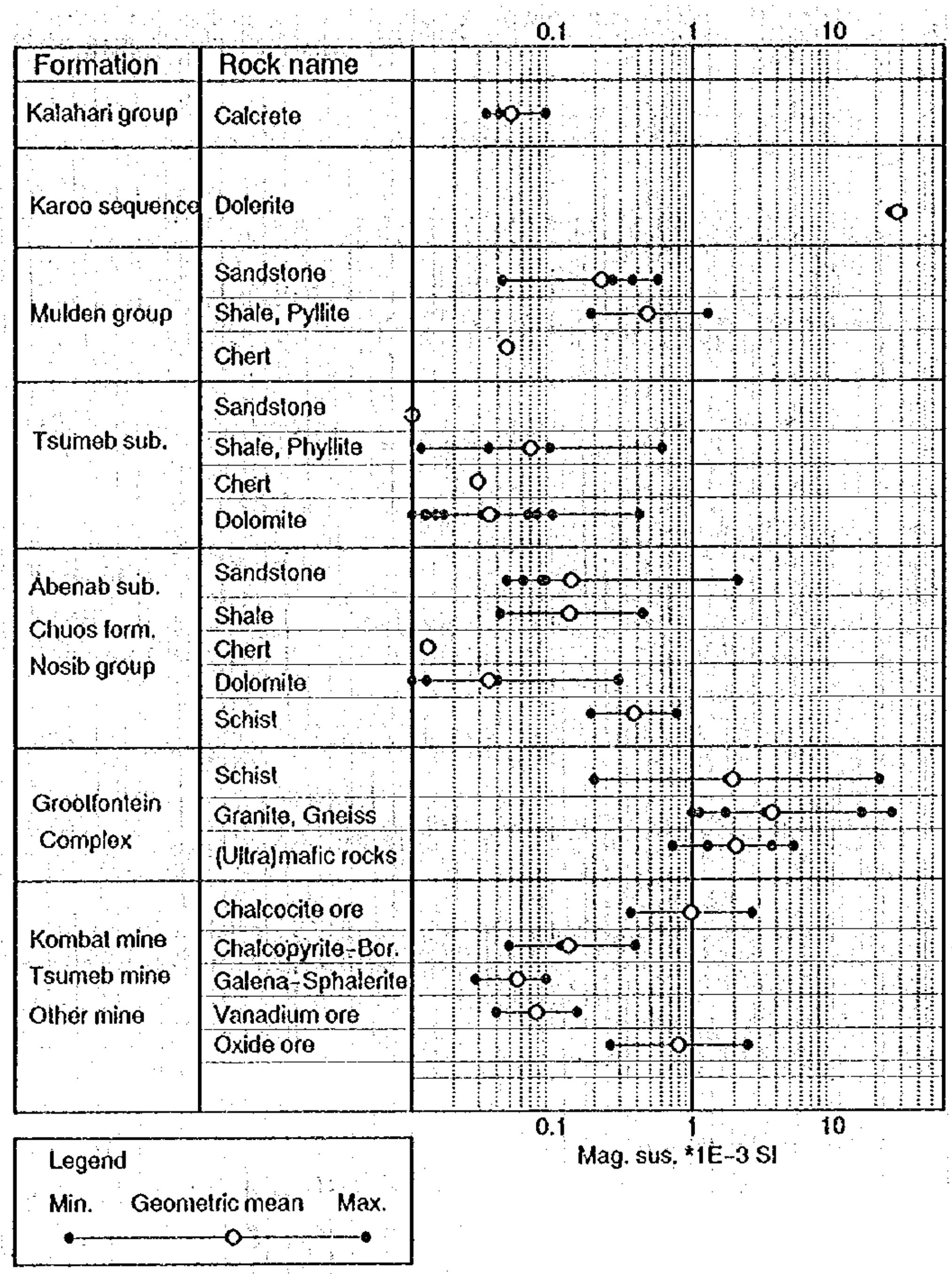

Fig. II – 4 – 7 Distribution of Magnetic Susceptibility

Zone	range	characteristics
Resistivity A	no more than 300 Ω ·m	massive sulphide.
Resistivity B	from 300 to 4,000 Ω ·m	disseminated ore minerals.
Resistivity C	4,000 Ω ·m more than 4,000 Ω ·m	Damara sequence
IP I	no less than 100mV/V	massive sulphide.
IP II	from 100 to 10mV/V	disseminated ore minerals
IP III	from 10 to 1mV/V	some ore minerals
		Metamorphic Complex
		Damara sequence
IP IV	less than 1 mV/V	dolomite and calcrete

The shale of Damara sequence and the ore (Chalcopyrite) are strongly anisotropic as suggested in Fig. II −4−8. The shales shows considerably lower values of resistivity parallel to bedding, compared to vertical to bedding where they are one forth to one tenth of value. The chalcopyrite ore from Kombat mine shows remarkable anisotropic properties.

In a specimen consisting of about equal portions of massive chalcopyrite and the hosting sandstone, low resistivity and high IP was measured when the current was introduced to the mineralized section, however, when the current was introduced across the sandstone/ore contact, higher resistivity by as much as tens times the former were recorded.

Generally, the more intensely a specimen is mineralized with sulphide, the lower resistivity and the higher IP may show. In the dolomites containing free carbon, high IP is anticipated and these carbonates are grouped into the above−mentioned IP III zone. However, it is thought that this will not affect the IP method for sulphide exploration.

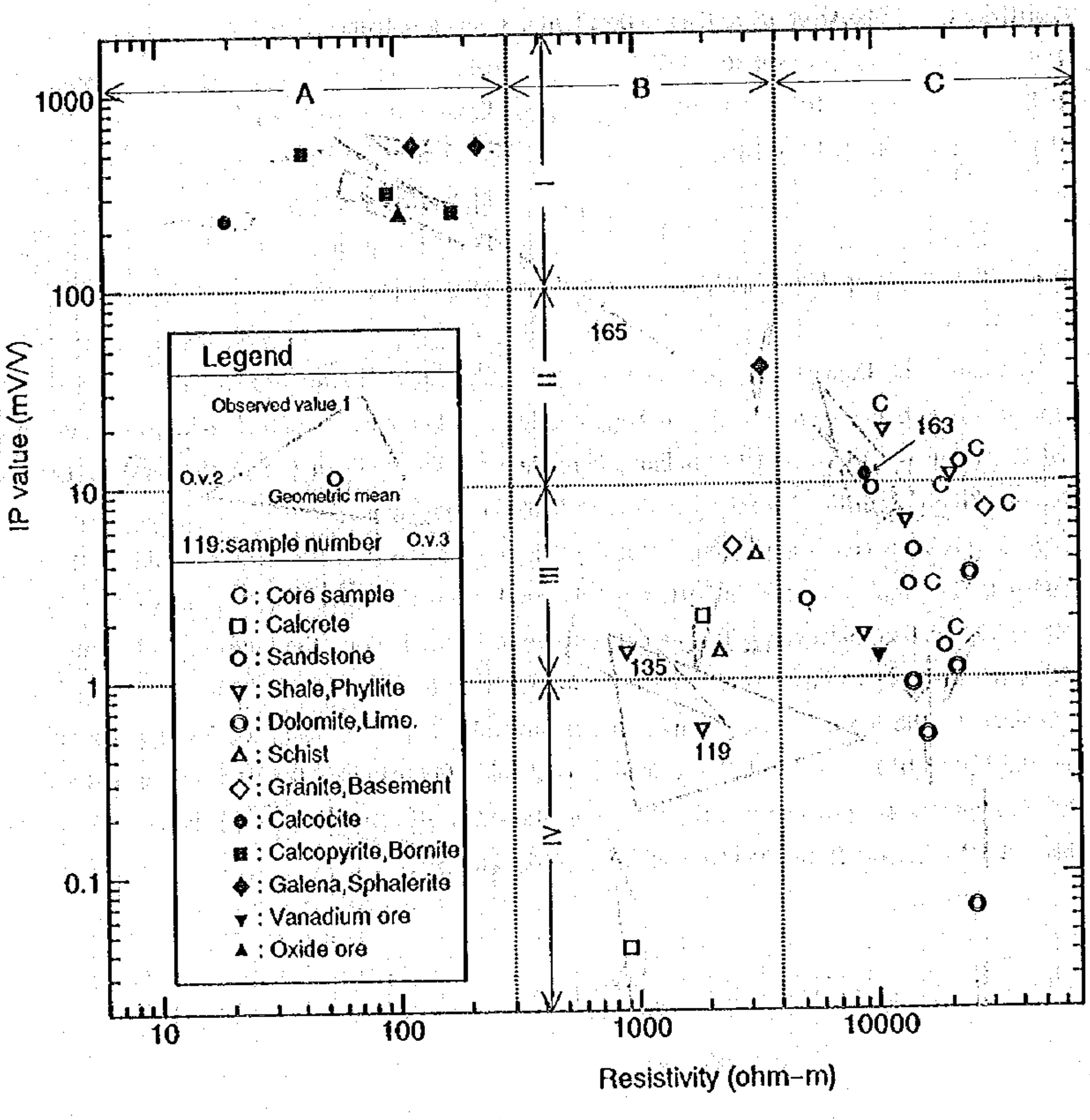

Fig. II − 4 − 8　Relationship between Resistivity and IP Value

Chapter 5 Radiometric Survey

II-5-1. Objective and Method

The main objective of a radiometric survey is to delineate subsurface radioactive rock units and interpret these for favorable ore hosting structures. The total gamma, K, Th and U intensity observed by gamma ray spectrometer are processed appropriately to extract fracture zones and to assume lithomaps.

II-5-2. Specifications

This the survey was carried out in conjunction with the aeromagnetic survey and the specifications are thus the same as those described in Table II-4-2.

II-5-3. Equipment

The equipment used are listed in Table II-4-1. The calibration of gamma ray spectrometer was done prior to the survey at the Eros airport calibration padsand again in Henties Bay.

II-5-4. Data Processing and Interpretation Procedure

Flow chart of the data processing and interpretation is illustrated in Fig. II-5-1.

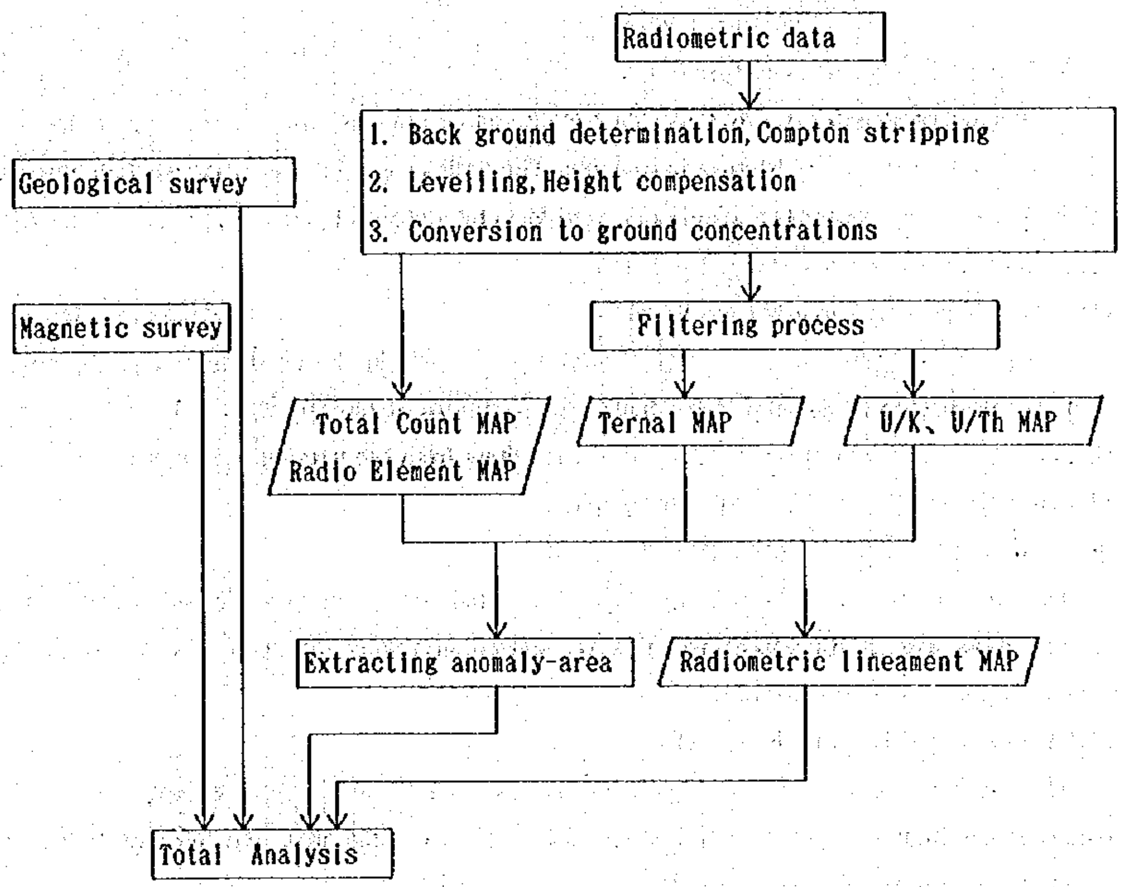

Fig. II-5-1 Flow Chart of the Aeroradiometric Survey

II-5-5. Result of Measurement and Interpretation

II-5-5-1. Result of Measurement

Total count radiometric anomaly map, Radiometric anomaly maps of K, Th and U radioelement and radiometric contour ternary map are shown in Fig. II-5-2, II-5-3, II-5-4, II-5-5 and II-5-6 respectively.

The radiometric contour ternary map is prepared through the overprint of each radiolement concentration to which a color assigned. The radiometric contour ternary map is prepared through overprinting of each radioelement concentration. Uranium and thorium counts were converted to equivalent contents whose minimum, maximum and mean values are shown below.

Element	Min.	Max.	Mean
K	0 %	2.9 %	0.2 %
eU	0 ppm	7.1 ppm	1.94 ppm
eTh	0.96 ppm	15.8 ppm	4.1 ppm

(The calculation was based upon 75 metre-grid interval.)

II-5-5-2. Interpretation and Discussion

Commonly radiometric surveys include exploration of uranium ore deposit, discrimination of lithofacies and extraction of fracture lineaments. The analysis and interpretation were emphasized on the last two objectives. The features derived form total count of gamma-ray and radioelement concentration maps are summarized as follows.

(1) Total gamma-ray anomaly (Fig. II-5-2)

The northeast-trending lineaments observed particularly in the northern half of the survey area are interpreted as fluvial paleochannels. Surfy pattern of anomaly identified east of the area seems to be paleodunes of the Kalahari desert resulting from the varying degree of concentration of each radioelement as well as paleotopography.

(2) Equivalent Uranium anomaly (Fig. II-5-3)

The uranium concentration is generally low and shows no specific anomalies. Weak concentration with northwestern trend is recognized in the central part where the thorium content is low. The northwest of the area is also anomalous.

(3) Thorium anomaly (Fig. II-5-4)

The thorium concentration is high over the exposed terrain as well as potassium and is comparatively high also in the central west and central part of the area. The concentration seems extend along with uranium concentration.

(4) Potassium anomaly (Fig. II-5-5)

The potassium content is higher over the exposed area than over calcrete terrain. Potassium concentration coincides conformably with the lithological boundary and Within the Damara sequence, the Abenab Subgroup in particular is more potassic. Within the Kalahari sand terrain, potassium is slightly high in the extreme northeast and low in the south. The anomaly map revealed that potassium was the important tool to discriminate the exposed lithofacies but in the terrain of calcrete.

Radon gas generated from uranium in depth may ascend through open fractures to the surface, therefore the linear anomaly of uranium provides useful information necessary for fracture mapping. Those fractures which are open up to the surface are believed considerably young in geologic time.

It is generally accepted that mineralisation may occur through the weak zones. Mineralisation of the area believed of the Mississippi Valley Type could be related to the linear structures that had enabled to form karsting at the loci of ore deposits. But it is quite difficult to clarify the relationship between the currently observed lineaments and ore deposits as stated above.

Such a large volume of detector as used in the survey may give high resolution but contemporaneously high level noise on the other hand. These noises show spiky kicks which are mechanically inevitable when small signals are detected and therefore the noise was removed by median filter resulting to the improvement.

The only anomaly originated from uranium could be extracted by means of U/K and U/Th ratios because these ratios of common rocks are less variable. U/K and U/Th ratio maps are shown in Fig. II −5−8 and Fig. II −5−9. In addition to the above−mentioned characteristics, the ratios are very important for the survey because of elimination of such radiometric disturbances as topography, artificial structure and meteorological change which may effect equally on a count of each radioelement.

Based upon the above mentioned figures the lineaments were extracted and illustrated in Fig. II −5−7, indicating the following aspects.

(1) A northeasterly trending radiometric lineament traverses close to the Abenab and Khusib ore deposits showing lithological extension.

(2) In the terrain of calcrete, a couple of weak but long lineaments were followed some of which are locally curved suggesting deformed older fracture zone. Those include chiefly west−northwesterly trending long lineaments running from the west to central of the surveyed area with some lineaments parallel to those.

(3) Weak but continuous lineaments strike northwesterly to the south of Abenab mine.

(4) Uncertain lineament

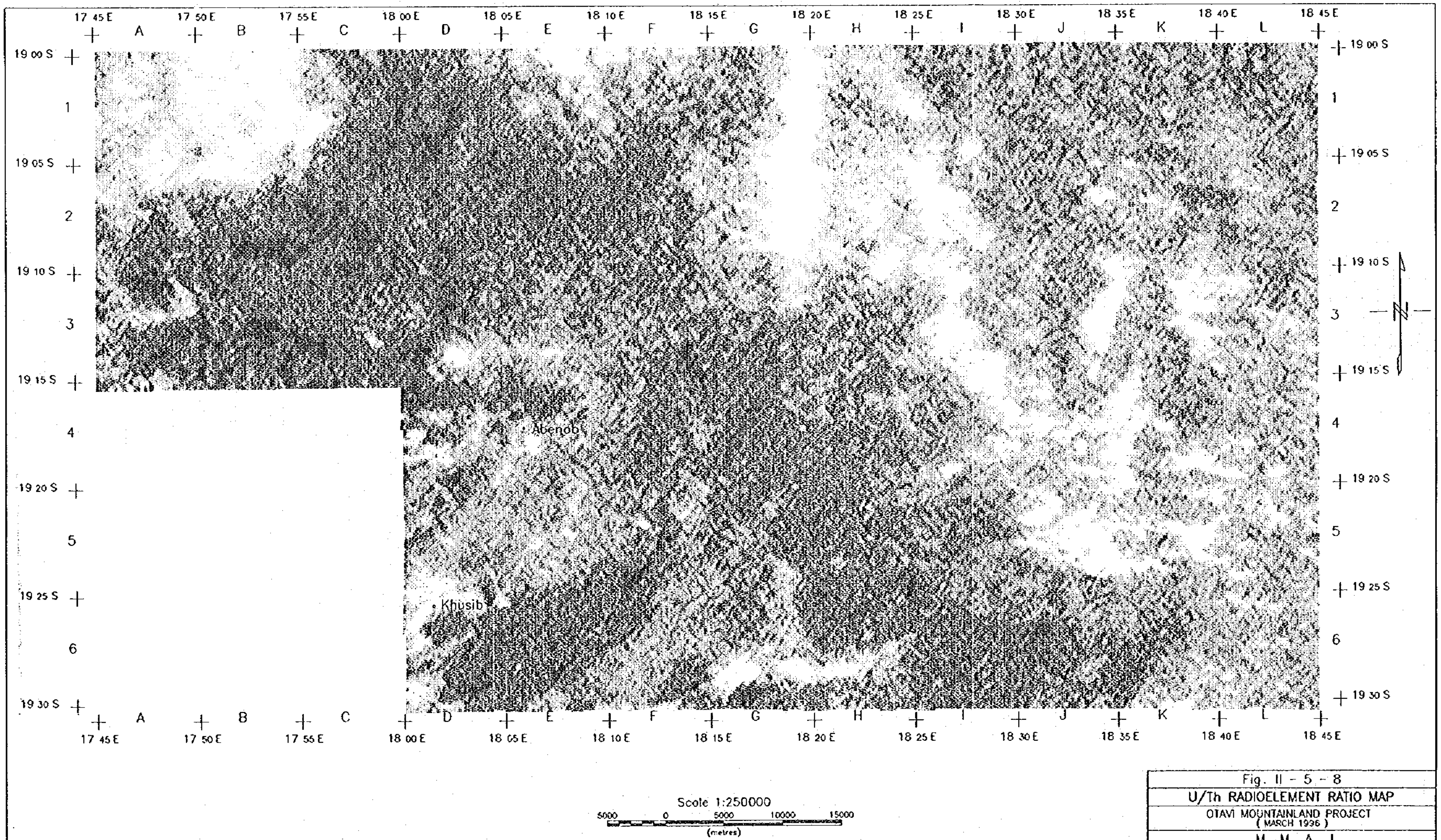

Fig. II - 5 - 8

U/Th RADIOELEMENT RATIO MAP

OTAVI MOUNTAINLAND PROJECT
(MARCH 1996)

M. M. A. J.

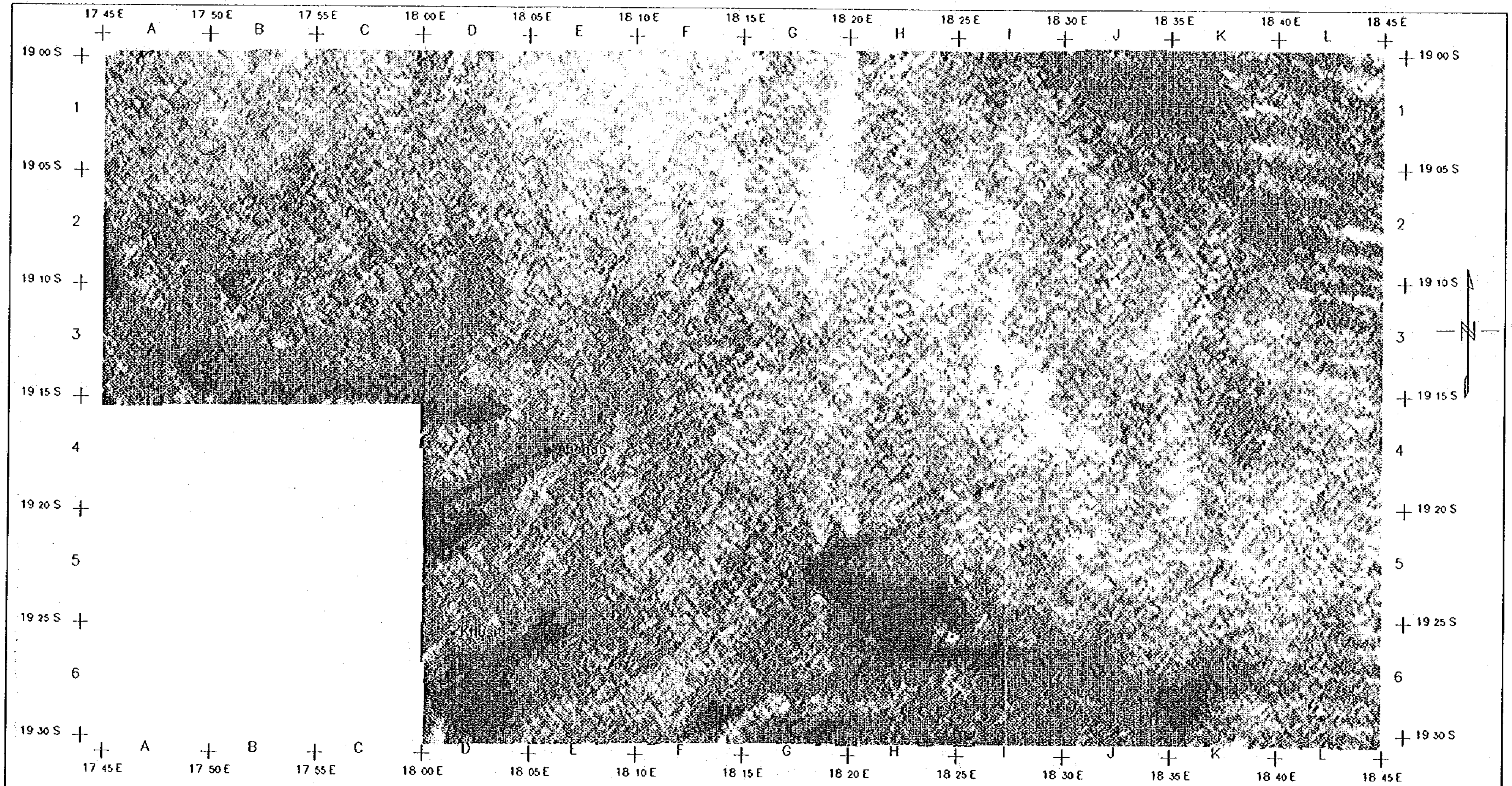

Scale 1:250000

5000 0 5000 10000 15000

(metres)

Fig. II - 5 - 9

U/K RADIOELEMENT RATIO MAP

OTAVI MOUNTAINLAND PROJECT
(MARCH 1996)

M. M. A. J.

The ore deposits in the Survey area include the Tsumeb and Kombat mines which are associated within feldspathic sandstone (Mulden Group) filled karst pipes that are developed in the upper part of Tsumeb Subgroup. The Mulden Group is believed to be sub aqueous or sub aerial molasses type sediments which was deposited unconformably on the Tsumeb Subgroup. Due to the different competencies of the lithofacies the folding initiated prior to Mulden period, has resulted in varying fold and fault patterns. Close to the surface, these fractures and faults facilitated percolation of meteoric water between the paleosurface and aquifer. Solution collapse breccias formed in the preexisting structural weaknesses of exploited by karsts. The karsts were filled with sands of the Mulden Group which was deposited before or during karst formation. The origin of the fracture system in a shallow depth is possibly relate to the folding such as intraformational slip faults and axial plane shearing.

However, deep seated fracture systems, acting as conduits for ascending fluid are of major importance for ore deposition. Such a deep seated faults are controlled by the structure of the basement complex. These basement structures have NE–SW striking trends in the metasediments of the basement complex, where as crosscutting dykes with NNE–SSW trending strikes, occur northwest of Grootfontein. Some of these deep seated faults may reach the paleosurface due to reactivation during the Damara Orogeny as this NE–SW trend coincides with the orientation of rifting during the initial deposition of Damara sequence. NNE–SSW trending lineaments are also recognized in the Pre–Damara basement. A northeast–striking, sub–outcropping dyke of olivine dolerite just west of the Tsumeb mine, and dykes and sills of kersantite in the mining area, provide evidence of post–ore magmatic activity.

However, earlier magmatism may also have occurred along this prominent linear structure. In addition to the above, aeromagneitc surveys in the Otavi Mountainland have indicated that the northeast–striking lineament is also manifested in the configuration of the basement rocks. Isopach studies undertaken by TCL have revealed that the lineament had been active during deposition of the Otavi Group. The lineaments or deep faults parallel to this lineament may have conducted heat from granitic intrusives farther to the southwest and the resulting convection systems could have driven metalliferous fluids into permeable structural loci.

The shallow seated fracture systems strike easterly, east northeasterly or west northwesterly and occasional northwesterly. At Kombat, it seems that the loci of ore deposit is controlled by east–northeast trending fractures which may correspond to crenulation cleavage formed during D2 period(500–570 Ma).

It is concluded that the loci of ore deposit may be controlled to the intersection of NE–SW or

NNE–SSW trending deep–seated fracture system with shallow seated E–W, WNW–ESE, ENE–WSW or NW–SE trending faults or fracture system. These intersections are therefore the prime exploration targets considered in the evaluation of the survey area.

The aeromagnetic survey revealed that the surveyed area could be divided into two zones by east–northeast to east trending lineaments. The southern half of the area is underlain by the basement complex at a shallow depth, whereas the northern half is overlain by thick carbonate pile of Damara sequence. The lineament gives two zones a significant magnetic contrast suggesting a possible deep–seated fault. The Abenab ore deposits are located close to the lineament, which may indicate close relation between the ore loci and that lineament. A couple of lineaments with northeast and north–northeast trends traverse the southern zone and the ore bodies of Khusib Springs appear to be associated with these. The Tsumeb ore deposit also seem to be emplaced close to northeast–trending lineaments which have associated dolerite dykes.

To the northeast of Grootfontein, the northeasterly trend of the lineaments shifts towards east–northeasterly. This change may be due to later stage deformation which is also recognized at Kombat and west of Tsumeb.

In the northern zone, the gentle relief of magnetic anomalies indicates domal structures of deep–seated basement rocks which are overprinted by a swarm of northwesterly trending lineaments that are possibly associated with intrusive rocks. These may be related to Karoo basaltic activity of post–ore age, but they could also be growth faults.

Another magnetic feature of the survey area is the quite faint magnetic contrast of the upper most Tsumeb Subgroup with the Mulden Group. This feature can be followed as continuous arcuate lineament and is an important exploration target as ore deposit may be hosted in karst below the unconformity.

The result of magnetic susceptibility tests indicate that the susceptibility of chalcocite mineralisation is high enough, compared to other ore minerals, in giving a weak but small distinctive circular magnetic anomaly if massively hosted by dolomite with a low magnetic susceptibility.

The Aeroradiometric survey indicated radioactive differences between lithofacies mainly in the area of rock outcrop. The Abenab and Khusib Springs deposits are situated close to a northeasterly trending radiometric lineament indicating a lithological boundary. This boundary corresponds to the contact between Damaran sedimentary rock and younger calcretes and coincides with the magnetic lineament which is concordant to the basement structure. This lineament therefore is interpreted as fracture zone controlled by faulting.

In the northwest of the surveyed area, some long locally curved lineaments with a northwest to east–west trend were recognized but the origin these is unclear.

Based upon the ore forming models, aeromagnetic and aeroradiometric lineaments, the ore potential of the surveyed area was evaluated, targeting massive sulphide pipe-like deposit and the following four criteria were used in the evaluation of potential targets:

(1) Proximity to unconformity (or disconformity, termed TM contact thereafter) of Mulden Group and synclinal crest or crest of secondary folding.

(2) Intersection of aeromagnetic and or aeroradiometric lineaments with northeastern trend and east-northeastern trend and TM contact.

(3) Important shift of the basement linear structure associated with TM contact nearby.

(4) Small aeromagnetic anomalies around TM contact

Criterion(1) supported by (2) and (3) was highly evaluated whereas criterion(4) was not used for its own. Seven subareas were thus chosen for high to moderate ore potential and these are shown in the table in increasing order of ore potential.

Subarea No.	Section	criteria	favorable features
1	G2 south	(2)	Intersection of NNW-trend dyke and WNW-trend dyke swarms traversing the TM contact
2	H3 north	(1)(4)	Small magnetic anomalies close to fold axis at TM contact
3	G3 central	(2)(3)(4)	Lineament shift of basement, from ENE to E-W Intersection of WNW-trend dyke and TM contact The dyke is associated with small magnetic anomaly Proximity of radiometric lineament
4	E3/E4 boundary	(1)(2)(4)	Magnetic lineament at fold axis Intersection of weak WNW and NNW-trend anomalies
5	D4 north	(2)(4)	Small magnetic anomaly of reverse magnetization
6	D3 central	(2)	Intersection of NE-trend fault associated with dyke and TM contact
7	B3 northeast	(1)(2)(4)	NNW-trend lineament duplicated with small magnetic anomaly

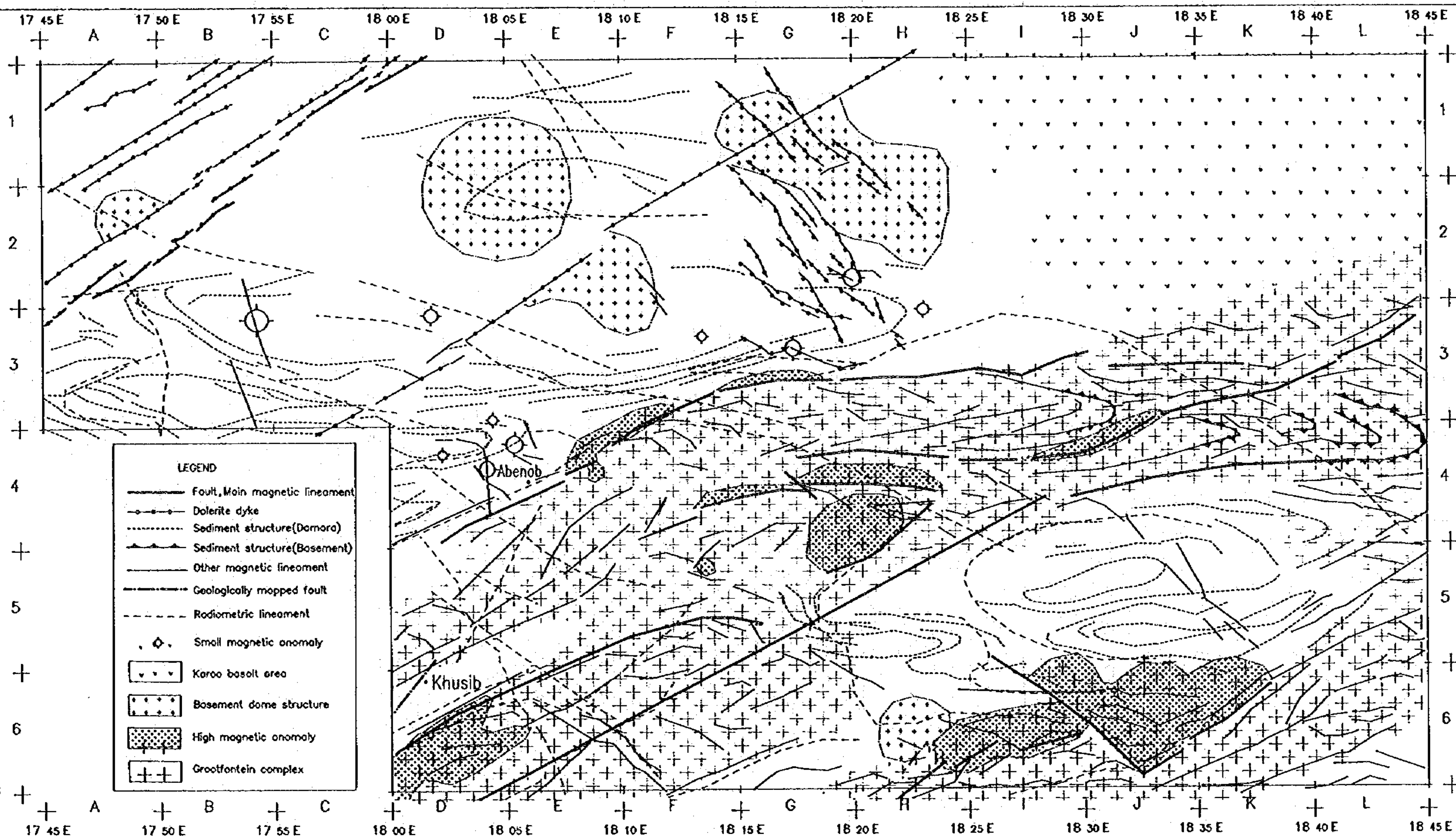

Scale 1:250000

5000 0 5000 10000 15000

(metres)

Fig. II - 6 - 1

COMPILATION AND INTERPRETATION MAP

OTAVI MOUNTAINLAND PROJECT
(MARCH 1995)

M. M. A. J.

Part III Conclusion and Recommendation

Part III Conclusion and Recommendation

Chapter 1 Conclusion

The survey of Phase I included research and compilation of the existing data, geological survey and airborne geophysical survey. The conclusion of the survey is summarized below.

1. Most of known ore deposits and mineralisation of the survey area are similar to those of so called Mississippi Valley Type ore deposits in some aspects.
2. The ore deposits are hosted in the Karst related sediments which filled caves formed in the carbonate rocks of Otavi Group of the upper Proterozoic Damara sequence.
3. The karst fill sediments, are principally permeable areneous' sediment and are related to sediments deposited unconformably on the carbonate rock. The permeability acts as conduit to mineralized fluids from depth.
4. The Damara sequence of the survey area was subject to several times of deformation to form multiple synclinorium and anticlinorium with east trending fold axis. The primary folding axis was deformed by later stage east-west compressional stress.
5. The fold structure and geometry of the basement complex are believed to be controlled by NE-SW or ENE-WSW trending faults.. These deep-seated faults and fracture system are important conduits for deep mineralized fluids.
6. The aeromagnetic survey indicated magnetic anomalies and magnetic lineaments that could be deep-seated faults which suggest that the basement complex extends into the area east of Grootfontein which is covered by calcrete of varying thickness.
7. The east and north of the area are covered by calcrete and are underlain by deep-seated basement complex and the thick carbonates of Damara sequence. The folding within the Mulden and Otavi Group could be delineated by to the faint difference in magnetic intensity.
8. The Radiometric lineaments coincide with magnetic lineaments and this indicates that those lineaments originated from the depth.
9. It seems that the known ore deposits are controlled by NE-SW trending lineament and fracture systems running west of Tsumeb and from Kombat through Harasib, Border, Khusib Spring to Abenab. In conjunction of the above the ore is controlled by intersection of various trend of fracture system related to folding. Particularly, of interest is that Tsumeb and Kombat are localized at the distorted crest of the primary synclinorium where NE-SW trending faults or fractures are duplicated.
10. The favorable areas for mineralisation were selected from the appraisal of aeromagnetic and aeroradiometric anomaly maps of areas covered by calcrete.

Chapter 2 Recommendation

Based upon the result of the survey and subsequent consideration and interpretation of all the data available, the following exploration programme for Phase II is recommended.

I-5-2-1. Survey area(Fig.II-6-1)

The location of the area is represented by the alphabetical letter combined with the number which are given to each section five by five minutes in the flown area. Seven subarea were selected for high to moderate ore potential in its increasing order as follows.

(1) G3 central area : Aregoas 282 Farm

(2) E3/E4 border area : Cleveland 706 Farm

(3) B3 northeast area : Aarhus 659 and Accra 660

(4) H3 north area : Guinab 277

(5) D4 north area : Cadix 678 and Christiana 705

(6) G2 south area : Vogelsang 284

(7) D3 central area : Demerara 699

I-5-2-2. Method

A massive copper-lead-zinc sulphide ore deposit is targetted. It may be of steeply emplaced pipe like-geometry underlying 50 metres to 100 metres deep from the surface. resistivity method using resistivity contrast between ore and host rock is most effective for search of such ore deposit. Taking the surface condition into consideration, Time Domain Electro Magnetic Method is the most favourable.

Coil disposition is of in loop capable of both vertical and horizontal surveys with loop size of 100 metres to 200 meters square for grid sampling.

Subsequent drilling exploration is also recommended when the result of the ground geophysical survey reveals favourable.

Bibliography

Corner B.(1983): An Interpretation of the Aeromagnetic Data Covering the Western Portion of the Damara Orogen in South West Africa/Namibia Spec. Publ.geol.Soc.S.Afr.,11(1983),339-354

Corner B.and W.A.Wilsher(1987):Proceedings of Exploration '87:Third Decennial In Geophysical and Geochemical Exploration for Minerals and Ground water, edited by G.D.Garland, Ontario Geological Survey, Special Volume 3, 960 p.

De Beer,J.H.et al(1982):Magnetometer array and deep Schlumberger soundings in the Damara orogen belt, South West Africa.Geophys. J.R.astr. Soc.,70,1982.11-29p.

Geological Survey of Namibia(1982):The Geology of South West Africa Namibia 1:1000000

Geological Survey of Namibia(1988):Geological Map of the Damara Orogen South West Africa/Namibia-1988 1:500 000

Geological Survey of Namibia(1993):Aeromagnetic Anomaly Map of Namibia 1: 1 000 000

Innes J. and Chaplin R.C.(1986):Ore Bodies of the Kombat Mine, South West Africa /Namibia. Mineral Deposits fo Southern Africa(1986),1789-1805p.

Japan Mining Engineering Center for International Cooperation(1992):Report on Project finding Survey-Satellite Image Interpretation, Republic of Namibia 1992 (in Japanese)

Japan Mining Engineering Center for International Cooperation(1992):Report on Project finding Survey-Information Analysis, Republic of Namibia 1992 (in Japanese)

Kileen P.G.(1979):Gamma Ray Spectrometric Methods in Uranium Exploration - Application and Interpretaion. Exploration '87 Proceedings-Geophysical Methods, Advances in the State of the Art. Geological Survey of Canada, Economic Geology Report 31,163-229p.,1979

Killick A.M.(1986):A Review of the Economic Geology of Northern South West Africa/Namibia. Mineral Deposits fo Southern Africa(1986),1709-1717p.

Kimura S.(1987):Localization of Spa using Surface Gamma-Ray Radiometric Exploration Spa Science Vol.37 1987 73-92p.(in Japanese)

Lombaard A.F., Gunzel A., Innes J.and Kruger T.L.(1986):The Tsumeb Lead-Copper-Zinc-Silver Deposit,South West Africa/Namibia. Mineral Deposits fo Southern Africa(1986),1761-1787p.

Miller R.McG.(1983):Economic Implications of Plate Tectonic Models of the Damara

Orogen. Spec. Publ. Geol. Soc. S. Afr., 11(1983), 385-395p.
Mining Journal :Country Supplement NAMIBIA Vol. 319 No. 8196 1992
Miller R. McG. (1994):The Mineral Resources of Namibia ---Mineral Exploration Targets
Niall M. and McMaus C. (1994):Proterozoic Crustal & Metallogenic Evolution. Abstracts. Geological Society & Geological Survey of Namibia
Tsumeb Corporation Limited(1995):Kombat Mine 1995
Welke H. J., Allsopp H. L. and Huges M. J. (1983):Lead Isotopic Studies Relating to the Genesis of the Base-Metal Deposits in the Owambo Basin, Namibia Spec. Publ. Geol. Soc. S. Afr., 11(1983), 321p.
Wolf K. H. edit. (1985):Handbook of Strata-Bound and Stratiform Ore Deposits, Vol. 5 Regional Studies, Vol. 6 Cu Zn Pb and Ag Deposits, Vol. 13 Regional Studies and Specific Deposits, ELSEVIER

A－1

PHOTOGRAPHS OF THE SURVEY AREA

A-1 Photographs of the Survey Area (1)

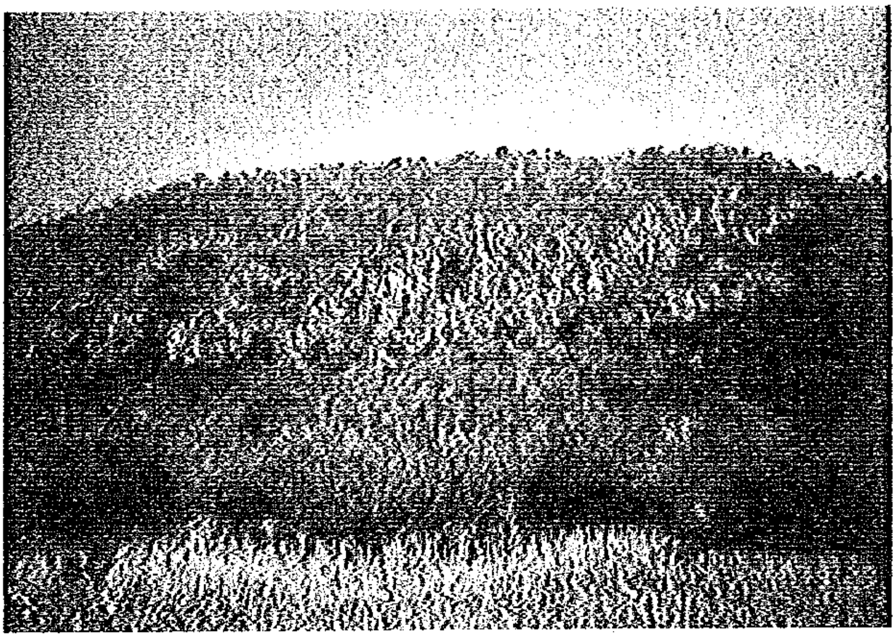

Common view of the Otavi Mountainland

Basement rock and dolomite

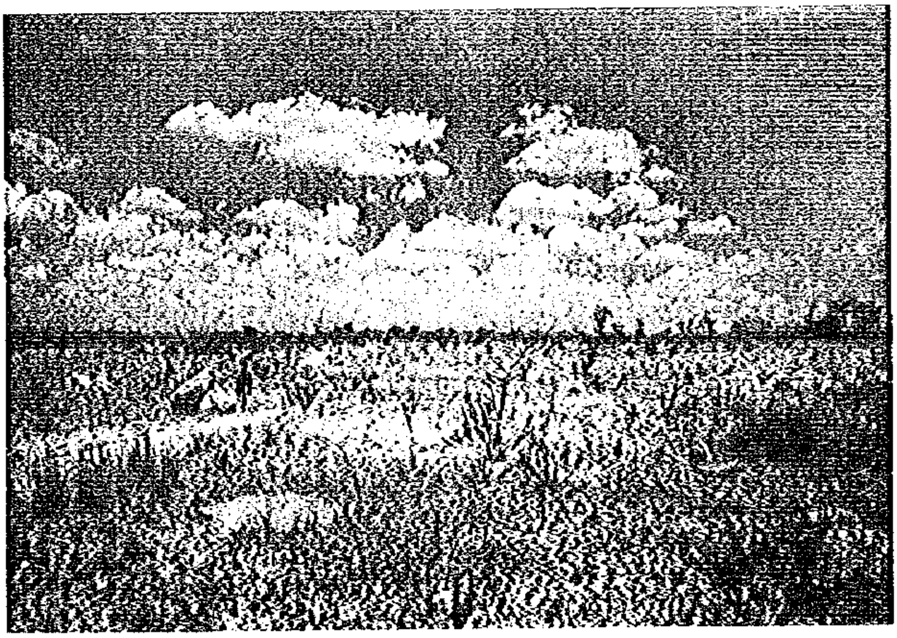

View of the flat land covered by calcrete

A-1 Photographs of the Survey Area (2)

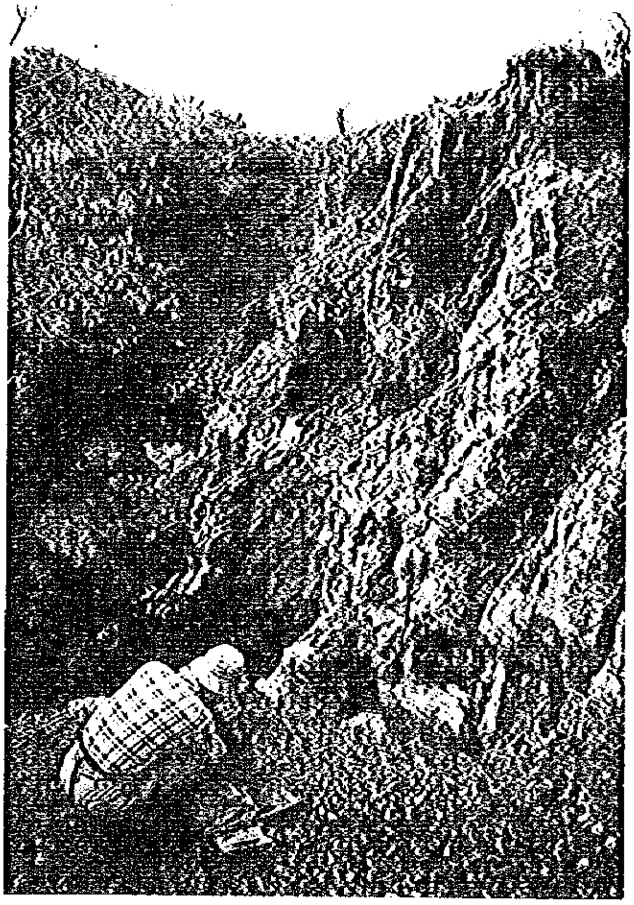

Sampling at the Bobos closed mine
southwest of Tsumeb

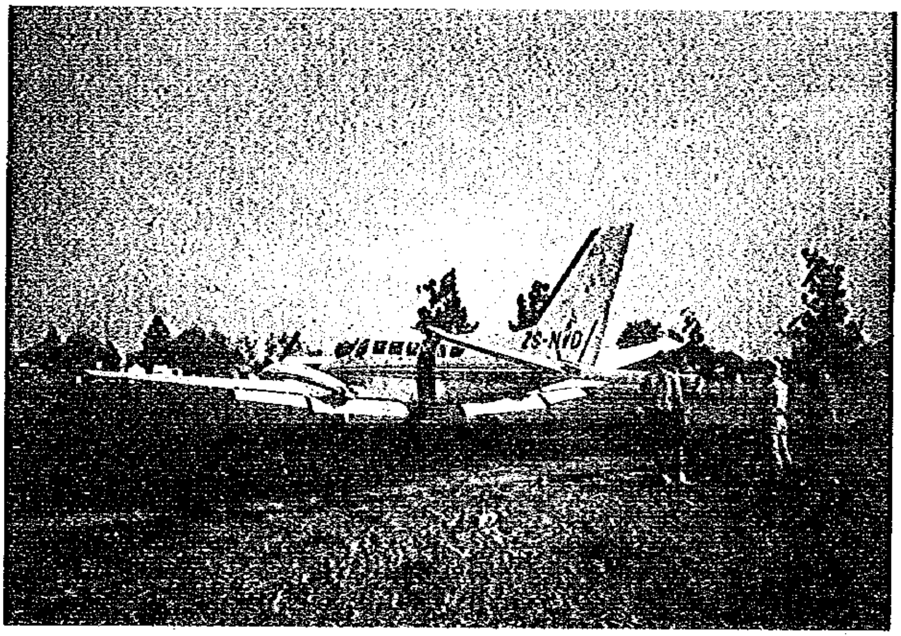

Airborne geophysical data acquisition by Cessna aircraft

A-2

MICROPHOTOGRAPHS OF THIN SECTION

Thin section photograph abbreviation

Minerals

Qz ——— quartz
Pl ——— plagioclase
Kf ——— potassium feldspar
Hb ——— horenblende
Mu ——— muscovite
Bi ——— biotite
Cal ——— calcite
Dol ——— dolomite
Ser ——— sericite
Chl ——— chlorite
Sp ——— sphene
Mt ——— magnetite
Zr ——— zircon
Ap ——— apatite
Tm ——— tourmaline
Lx ——— leucoxene
Ep ——— epidote
Hm ——— hematite
Op ——— opaque mineral

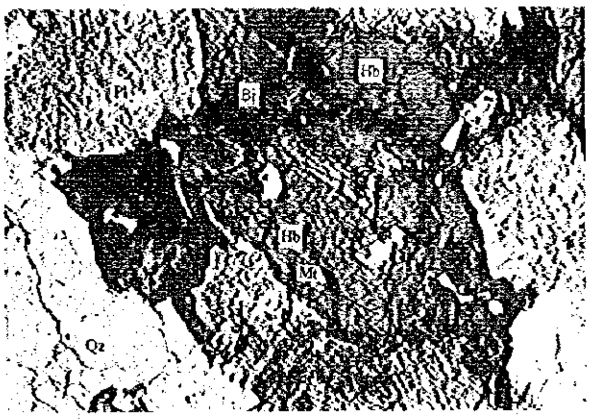

Sample No. 100504 Open Nicol

Formation Grootfontein Metamorphic Complex 0 0.5mm

Rock Name Biotite-hornblende-granodiorite

Locality Nosib Block 111

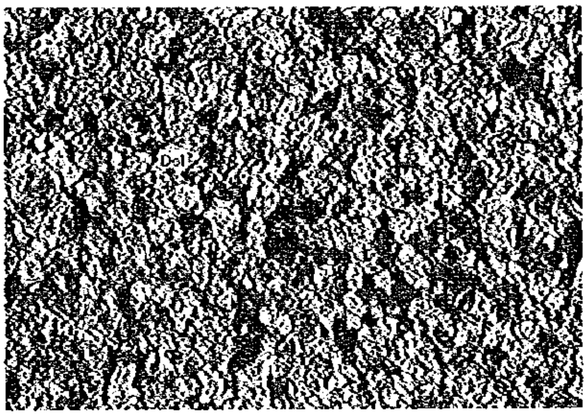

Sample No. 110705 Open Nicol

Formation Tsumeb Subgroup

Rock Name Dolomite

Locality Tsumeb Mine

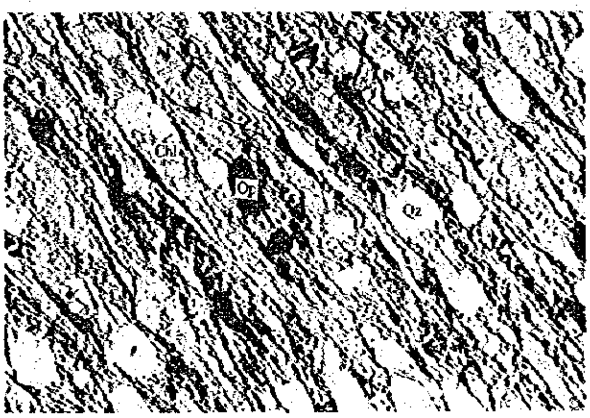

Sample No. 101308 Open Nicol

Formation Chuos 0 0.5mm

Rock Name Quartz-chlorite schist

Locality Askevold

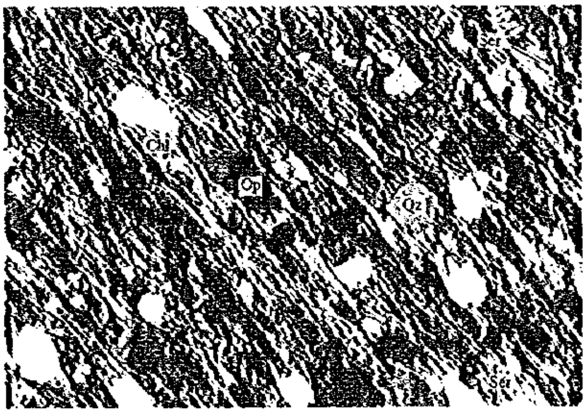

Cross Nicol

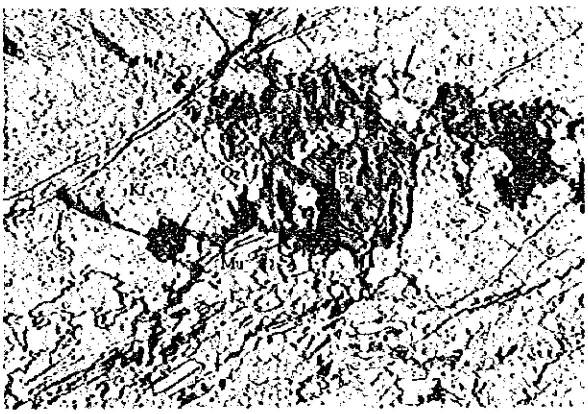

Sample No. 102103 Open Nicol

Formation Grootfontein Metamorphic Complex 0 0.5mm

Rock Name Biotite-muscovite granite

Locality Rietfontein

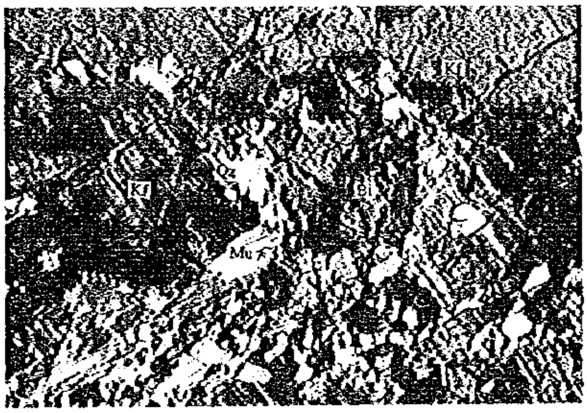

Open Nicol

A－3

MICROPHOTOGRAPHS OF POLISHED SECTION

Polish photograph abbreviation

Minerals

Cp ——— Cuprite

Gn ——— Galena

Sp ——— Sphalerite

Py ——— Pyrite

Cc ——— Chalcocite

Bo ——— Bornite

Nc ——— Native cupper

Cup ——— Cuprite

Dg ——— Digenite

Cv ——— Coveline

V ——— Descloizite or mottramite

Fe ——— Fe hydroxide

M ——— Malachite

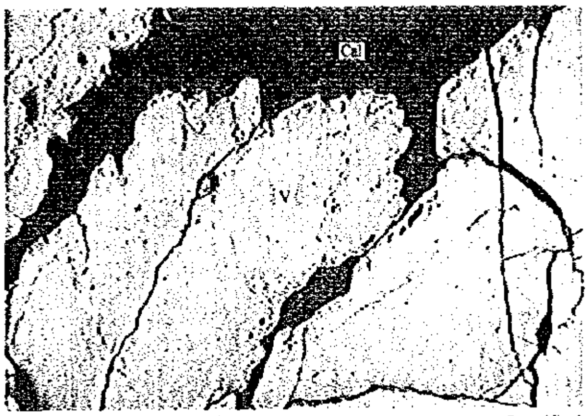

Sample No. 100405 | Open Nicol
Ore Name Vanadium ore | 0 0. 2mm
Locality Bobos mine(closed)

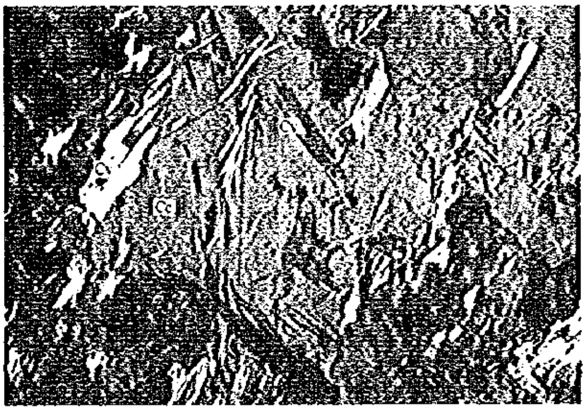

Sample No. 101104 | Cross Nicol
Ore Name Chalcocite-covelline ore | 0 0. 2mm
Locality Rodgerberg mine(closed)

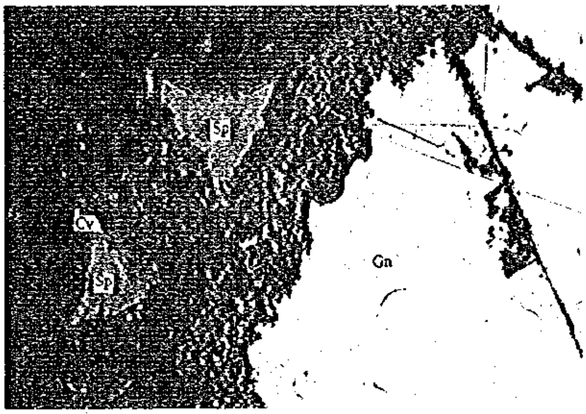

Sample No. 102006 | Open Nicol
Ore Name Galena-sphalerite ore | 0 0. 2mm
Locality Harasib old digging

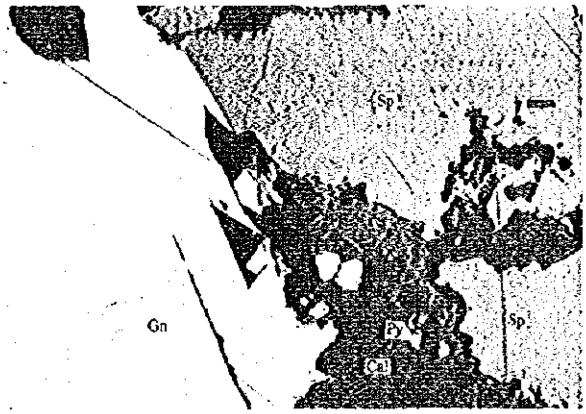

Sample No. 102501 | Open Nicol
Ore Name Sphalerite-galena ore | 0 0. 2mm
Locality Abenab mine(closed)

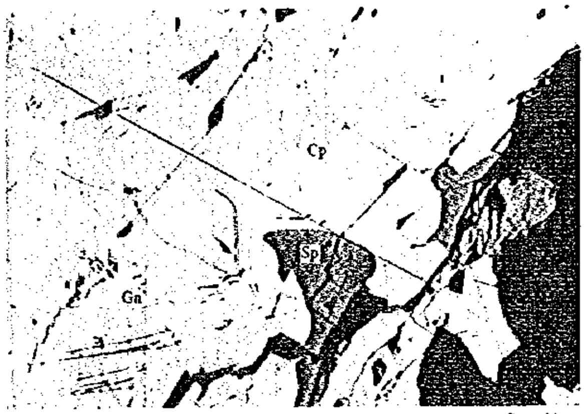

Sample No. 110604 | Open Nicol
Ore Name Galena-chalcopyrite ore | 0 0. 2mm
Locality Kombat mine 16L/1 No. 2

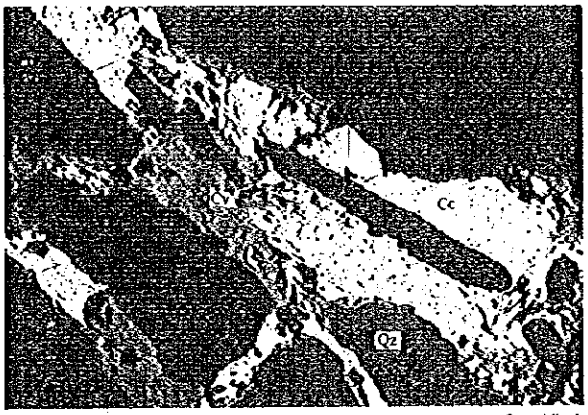

Sample No. 110701 | Open Nicol
Ore Name Chalcocite-covelline ore
Locality Tsumeb mine L10 No. 1

THE MINERAL EXPLORATION
IN THE OTAVI MOUNTAIN LAND AREA
THE REPUBLIC OF NAMIBIA

PHASE I

Fig. II-2-3

Location Map of
Known Mineral Showings

SCALE	1:250,000
JAPAN INTERNATIONAL COOPERATION AGENCY METAL MINING AGENCY OF JAPAN	
DATE	MARCH 1996

LEGEND

× Producing mine

× Closed mine

● ⑮ Old digging/ Mineral showing
Location number corresponds to the head number of Table II-2-2

Harasib:
Farm Name of Mineral Occurrence and Previous Exploration

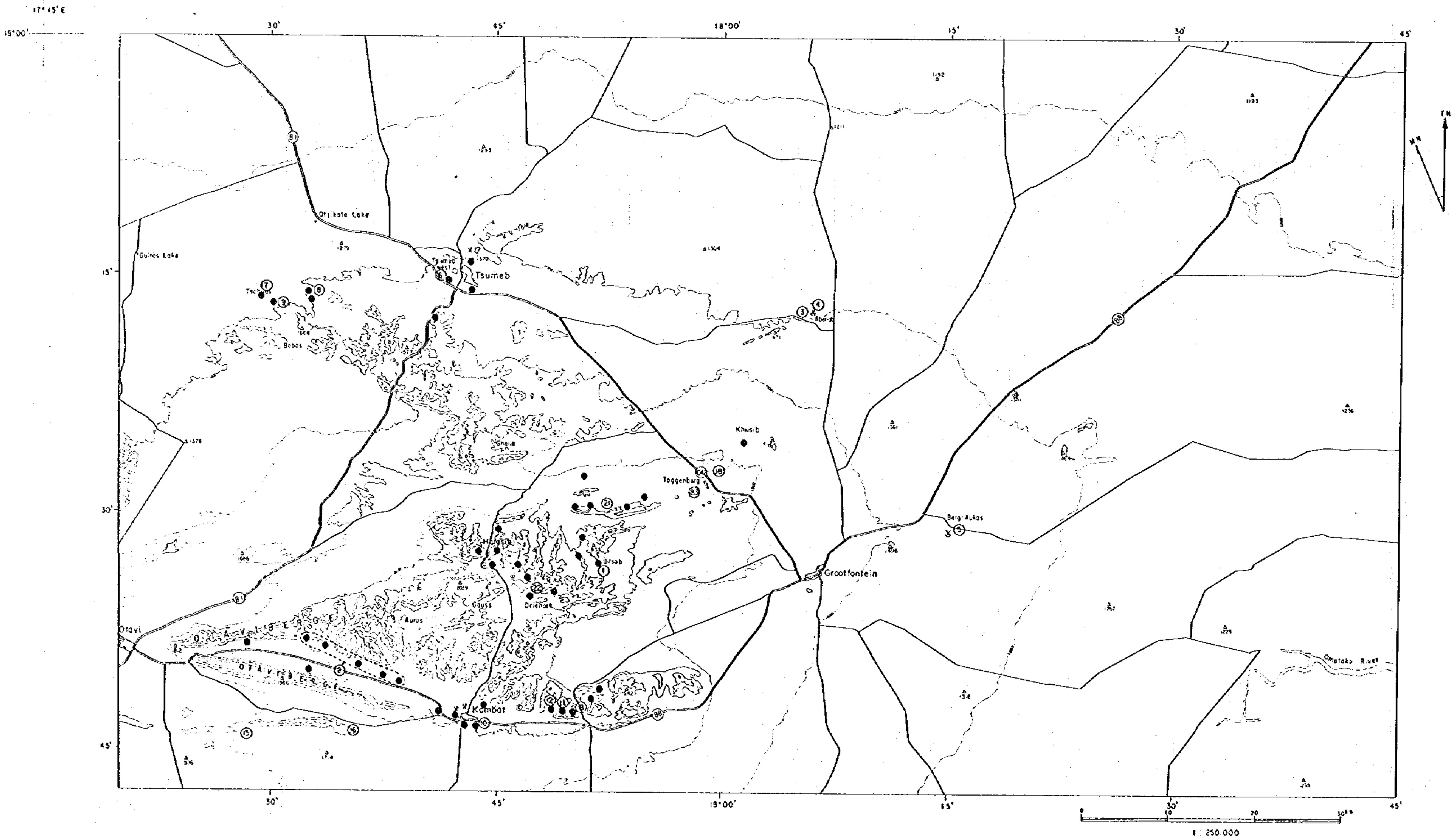

LEGEND

		FORMATION	SUBGROUP	GROUP	SEQUENCE COMPLEX
Tk	Alluvium, aeolian sand, gravel, calcrete			KALAHARI	
Nm	Quartzite, greywacke, conglomerate, phyllite			MULDEN	DAMARA SEQUENCE
Nt	Dolomite, limestone, chert, phyllite		TSUMEB	OTAVI	
Nc	Tillite, quartzite	CHOUS			
Na	Dolomite, limestone, shale		ABENAB		
Nk	Schist	KUISEB		SWAKOP	
Nkb	Marble, calc-silicate	KARIBIB			
Nc	Tillite	CHOUS			
Nas	Epidosite, agglomerate, chlorite schist, dolomite	ASKEVOLO		NOSIB	
Nv	Tillite, pyroclastics, ironstone	VARIANTO			
Nn	Quartzite, arkose, conglomerate, shale, phyllite				
Mgr	Granite, gneiss				GROOTFONTEIN MENTAMORPHIC COMPLEXEX

This Map was prepared on the basis of the Geological Map kindly presented by Tsumeb Corporation Limited under a grant of the Director of The Geological Survey of Namibia.

- Main Road
- Local Road
- Contour (Interval 100m)
- Town
- Mine
- Closed Mine
- Mineral Occurrence
- Strike Dip
- Fault
- Thickness of Calcrete
- Cross Section

LEGEND (Geologic Cross Section)

- Mulden Group
- Tsumeb Subgroup } Otavi Group
- Abenab Subgroup } Otavi Group
- Nosib Group
- Grootfontein Metamorphic Complex

THE MINERAL EXPLORATION
IN THE OTAVI MOUNTAIN LAND AREA
THE REPUBLIC OF NAMIBIA

PHASE I

Fig. II-3-2

Compiled Geologic Map

SCALE	1 : 250, 000

JAPAN INTERNATIONAL COOPERATION AGENCY
METAL MINING AGENCY OF JAPAN

DATE	MARCH 1996

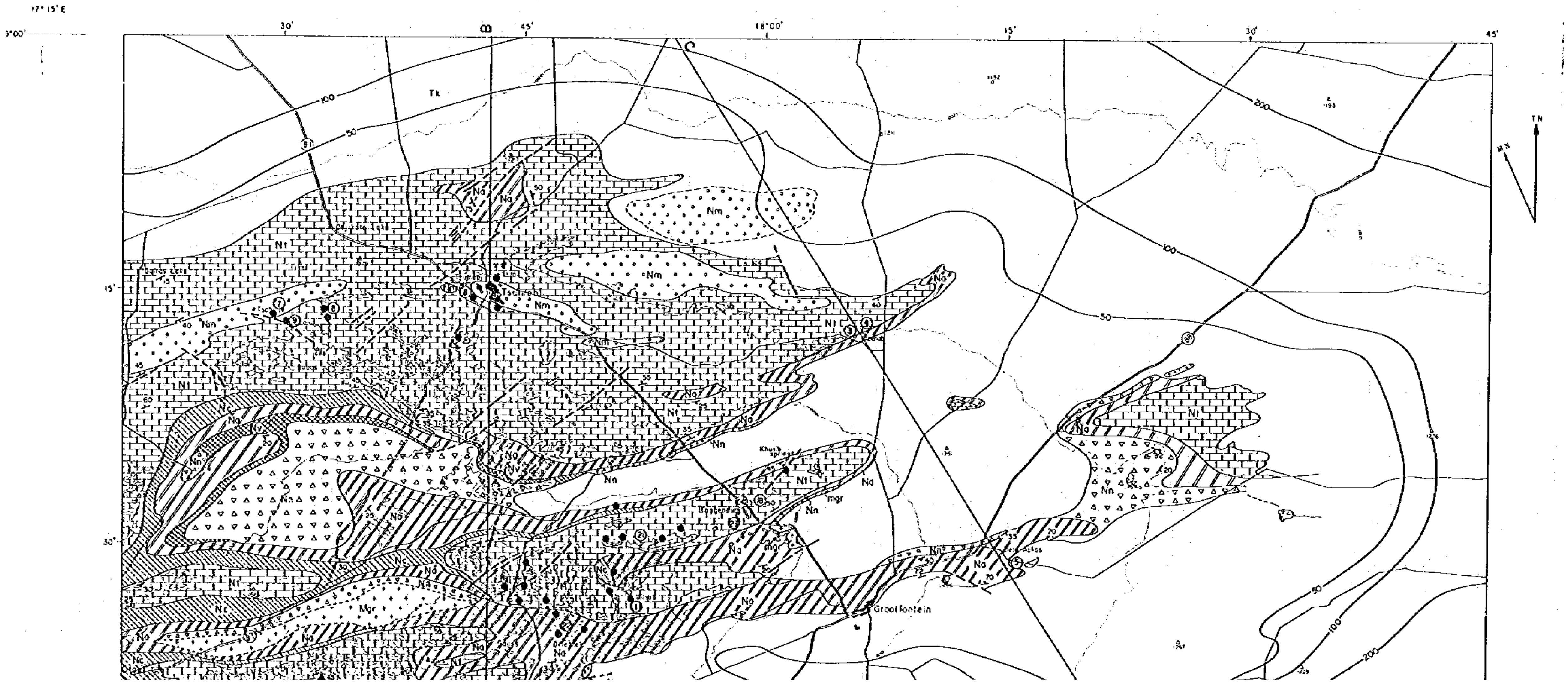

Geologic Cross Section

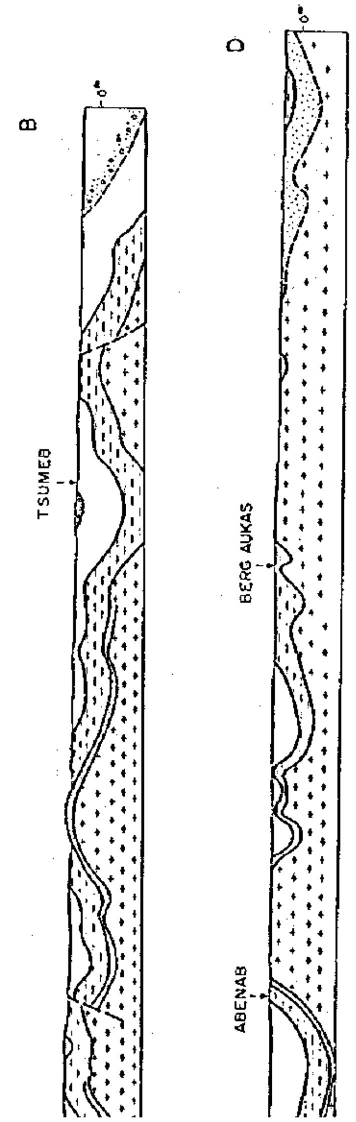

Nkb	Marble, calc-silicate	KARIBIB	SWAKOP	DAMARA SEQUENCE
Nc	Tillite	CHOUS		
Nos	Epidosite, agglomerate, chlorite schist, dolomite	ASKEVOLD	NOSIB	
Nv	Tillite, pyroclastics, ironstone	VARIANTO		
Nn	Quartzite, arkose, conglomerate, shale, phyllite			
Mgr	Granite, gneiss			GROOTFONTEIN MENTAMORPHIC COMPLEXEX

This Map was prepared on the basis of the Geological Map kindly presented by Tsumeb Corporation Limited under a grant of the Director of The Geological Survey of Namibia.

- Local Road
- Contour (Interval 100m)
- Town
- Mine
- Closed Mine
- Mineral Occurrence
- Fault
- Thickness of Calcrete
- Cross Section

- Tsumeb Subgroup } Otavi Group
- Abenab Subgroup } Otavi Group
- Nosib Group
- Grootfontein Metamorphic Complex

Compiled Geologic Map

SCALE	1 : 250, 000
JAPAN INTERNATIONAL COOPERATION AGENCY METAL MINING AGENCY OF JAPAN	
DATE	MARCH 1996

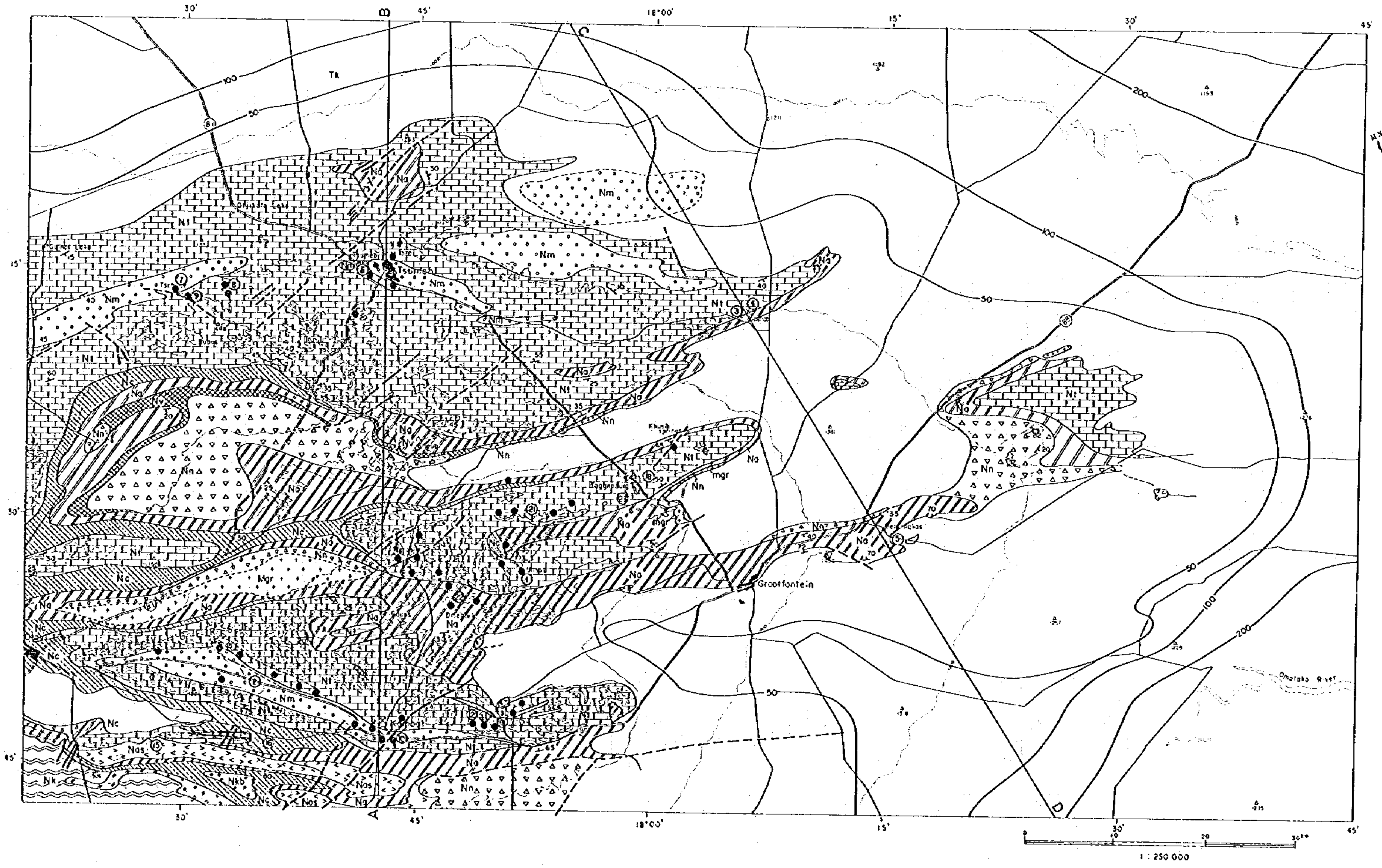

Geologic Cross Section